MCB
Journals.ASM.org

# Glucose Oxidation Modulates Anoikis and Tumor Metastasis

**Sushama Kamarajugadda,[a] Lauren Stemboroski,[a] Qingsong Cai,[a] Nicholas E. Simpson,[b] Sushrusha Nayak,[c] Ming Tan,[d] and Jianrong Lu[a]**

Departments of Biochemistry and Molecular Biology,[a] Medicine,[b] and Pediatrics,[c] University of Florida College of Medicine, Gainesville, Florida, USA, and Mitchell Cancer Institute, University of South Alabama, Mobile, Alabama, USA[d]

**Cancer cells exhibit altered glucose metabolism characterized by a preference for aerobic glycolysis or the Warburg effect, and the cells resist matrix detachment-induced apoptosis, which is called anoikis, a barrier to metastasis. It remains largely unclear whether tumor metabolism influences anoikis and metastasis. Here we show that when detached from the matrix, untransformed mammary epithelial cells undergo metabolic reprogramming by markedly upregulating pyruvate dehydrogenase (PDH) kinase 4 (PDK4) through estrogen-related receptor gamma (ERRγ), thereby inhibiting PDH and attenuating the flux of glycolytic carbon into mitochondrial oxidation. To decipher the significance of this metabolic response, we found that depletion of PDK4 or activation of PDH increased mitochondrial respiration and oxidative stress in suspended cells, resulting in heightened anoikis. Conversely, overexpression of PDKs prolonged survival of cells in suspension. Therefore, decreased glucose oxidation following cell detachment confers anoikis resistance. Unlike untransformed cells, most cancer cells demonstrate reduced glucose oxidation even under attached conditions, and thus they inherently possess a survival advantage when suspended. Normalization of glucose metabolism by stimulating PDH in cancer cells restores their susceptibility to anoikis and impairs their metastatic potential. These results suggest that the Warburg effect, more specifically, diminished glucose oxidation, promotes anoikis resistance and metastasis and that PDKs are potential targets for antimetastasis therapy.**

Aberrant energy metabolism is a widespread cancer-associated trait (13). Altered glucose metabolism is the best-characterized metabolic phenotype of cancer cells. Cells metabolize glucose to pyruvate through glycolysis. In normal tissues under aerobic conditions, glycolysis-derived pyruvate is primarily oxidized to acetyl coenzyme A (CoA) in mitochondria, which then enters the tricarboxylic acid (TCA) cycle to produce reducing equivalents for efficient generation of ATP through oxidative phosphorylation (OXPHOS). Under anaerobic conditions, pyruvate is diverted away from mitochondria and is reduced to lactate, which is excreted from the cell (17, 27, 32). Compared with normal cells, cancer cells consume much more glucose through increased glucose uptake and glycolysis. Moreover, even in the presence of oxygen, most pyruvate resulting from glycolysis in cancer cells is converted to lactate instead of entering the mitochondrial oxidation pathway. A cancer cell's preference for aerobic glycolysis rather than mitochondrial oxidation is known as the Warburg effect (18).

Cancer is a genetic disease caused by dysregulation of various signaling pathways that orchestrate cell growth and survival. A few key pathways that drive tumorigenesis can reprogram cellular metabolism and promote aerobic glycolysis (4, 14, 19, 20, 34). Although the alterations in glucose metabolism are nearly universal in tumors, there has been controversy over whether they are a by-product of the transformation process or a functional contributor to the development of malignancy. It is now widely recognized that the Warburg effect provides anabolic support and hence a selective growth advantage for cancer cells (34). Cell proliferation requires not only ATP but also synthesis of nucleotides, lipids, and proteins (34). Aerobic glycolysis in cancer cells generates large quantities of various carbohydrate metabolites that can be shunted into multiple biosynthetic pathways. The glycolytic intermediates glucose-6-phosphate, fructose-6-phosphate, and glyceraldehyde-3-phosphate can be converted to ribose-5-phosphate for nucleotide synthesis; 3-phosphoglycerate, phosphoenolpyruvate, and pyruvate can produce nonessential amino acids. Through the pentose phosphate pathway (PPP), glucose-6-phosphate gives rise to NADPH, which is required for the synthesis of fatty acids. Therefore, elevated glycolysis in cancer cells offers sufficient precursor metabolites to meet the increased anabolic needs of the rapidly dividing cells (34).

This notion is further exemplified by recent discoveries that the phosphoglycerate dehydrogenase (*PHGDH*) gene, which encodes an enzyme to direct 3-phosphoglycerate into synthesis of serine and glycine, is amplified in human cancers and contributes to cancer cell proliferation (22, 29).

In addition to being highly proliferative, cancer cells are refractory to apoptosis, including anoikis, a type of apoptotic cell death caused by inadequate or inappropriate cell-matrix interactions (8). Integrin-mediated attachment to the extracellular matrix (ECM) activates prosurvival signaling pathways (e.g., the phosphatidylinositol 3-kinase [PI3K]–AKT cascade) (25). Matrix detachment in normal cells leads to the loss of survival signals and triggers both extrinsic and intrinsic apoptotic pathways. The latter includes activation of BH3-only proapoptotic proteins, such as Bim, Bmf, and Bid (11), resulting in mitochondrial outer membrane permeabilization (MOMP), release of cytochrome *c* and other proapoptotic factors, and consequently caspase activation and apoptosis (33). Furthermore, matrix detachment causes an increase in the level of reactive oxygen species (ROS) in endothelial cells and mammary epithelial cells (21, 31). Because of their

**Received** 7 September 2011 **Returned for modification** 7 November 2011
**Accepted** 10 March 2012
**Published ahead of print** 19 March 2012
Address correspondence to Jianrong Lu, jrlu@ufl.edu.

doi:10.1128/MCB.06248-11

oxidative nature, excessive ROS can damage cellular components. Through multiple mechanisms, ROS stimulate the release of apoptosis-inducing factors, including cytochrome *c* from mitochondria, and subsequent activation of the caspase cascade and cell death (26). Further oxidation of cytochrome *c* by ROS potentiates its proapoptotic activity (35).

Resistance to anoikis is crucial in particular for the metastatic spread of cancer cells (25). Upon detachment from the primary site, cancer cells are displaced from their original matrix components. Following intravasation, circulating cancer cells in the bloodstream are deprived of ECM. After extravasation, disseminated cancer cells are exposed to foreign matrix niches at secondary sites. Therefore, during the metastatic process, cancer cells are in a dynamic state lacking stable matrix environments. Anoikis is thus an important barrier to metastasis. The ability of malignant cells to survive independently of anchorage is an essential prerequisite for successful dissemination.

Cancer cells exhibit both altered energy metabolism and resistance to anoikis, but the potential mechanistic link between them remains poorly understood. Recently, it has been found that matrix attachment profoundly influences cellular metabolism. Detachment of untransformed mammary epithelial cells from ECM reduces glucose uptake and hence the PPP (31). This leads to decreased antioxidant capacity and increased oxidative stress. The latter inhibits fatty acid oxidation (FAO) and consequently causes ATP deficiency (31). Antioxidants restore ATP generation by stimulating FAO. Impaired ATP production due to matrix detachment can be rescued by the ERBB2/HER2 oncoprotein (31).

In the present study, we explored the potential impact of glucose metabolism on a cell's sensitivity to anoikis. We show that upon matrix detachment, untransformed human mammary cells upregulate pyruvate dehydrogenase kinase 4 (PDK4) through the orphan nuclear receptor estrogen-related receptor gamma (ERRγ). PDK4 phosphorylates and inactivates pyruvate dehydrogenase (PDH), which is required for the conversion of pyruvate to acetyl-CoA. Therefore, cell detachment reprograms glucose metabolism by attenuating the flow of glycolysis-derived pyruvate into mitochondrial oxidation. Importantly, this metabolic response reduces mitochondrial ROS production and prolongs cell viability specifically in the absence of matrix attachment. Therefore, glucose metabolism is a determinant factor modulating anoikis sensitivity, and decreased glucose oxidation confers anoikis resistance. Cancer cells, due to the Warburg effect, constitutively exhibit decreased oxidative metabolism of glucose and are thus expected to inherently possess a survival advantage in suspension. Reverting the Warburg metabolic phenotype by stimulating glucose oxidation in cancer cells restores their sensitivity to anoikis and impairs their metastatic potential. These observations firmly implicate the Warburg effect in tumor metastasis and suggest that the altered glucose metabolism in cancer cells contributes to malignancy by conferring both growth and survival advantages on cancer cells. The study suggests that metabolic modulation may be a viable therapeutic approach to treat metastasis.

## MATERIALS AND METHODS

**Cells and reagents.** MCF10A (untransformed human mammary epithelial cell line), HMEC (human mammary epithelial cells), and SKMEL-5 (melanoma cells) were purchased from ATCC. MDA-MB-231 was a kind gift from Kevin Brown (University of Florida). MCF10A and HMEC cells were cultured in Dulbecco' modified Eagle medium (DMEM)–F-12 medium (Cellgro) supplemented with 5% horse serum (Sigma), 20 ng/ml epidermal growth factor (EGF; Sigma), 10 μg/ml insulin (Sigma), 0.5 μg/ml hydrocortisone (Sigma). MDA-MB-231 cells were grown in DMEM (Cellgro) supplemented with 10% fetal bovine serum. All assays in untransformed and cancer cells were performed 24 h and 48 h, respectively, after incubation under attached and suspended conditions unless otherwise noted. The antioxidants L-glutathione (GSH) and α-lipoic acid were purchased from Sigma.

**Plasmids and site-directed mutagenesis.** Full-length cDNAs of PDHE1α and PDK1, -2, -3, and -4 were obtained from OpenBiosystems. PDHE1α cDNA was amplified by PCR with a carboxyl-terminal Flag tag and cloned into the lentiviral expression vector pCSCGW2. Site-directed mutagenesis of PDHE1α was carried out by PCR with the following primers: S232A, forward, 5′-TGGAATGGGAACAGCTGTTGAGAGAGCGGCAGCC-3′, and reverse, 5′-CTCTCTCAACAGCTGTTCCCATTCCATAGCGATT-3′; S293, 300A, forward, 5′-TACCACGGACACGCCATGAGTGACCCGGGAGTCGCTTACCGTACACGAGAAGAAATT-3′, and reverse, 5′-CGTGTACGGTAAGCGACTCCCGGGTCACTCATGGCGTGTCCGTGGTAACGGTA-3′.

**Northern blotting and quantitative RT-PCR.** Total RNA isolation from cells grown under attached and suspended conditions was carried out with TRIzol (Invitrogen), following the manufacturer's protocol. Ten micrograms of RNA of each sample was used for Northern blotting with $^{32}$P-labeled PDK4 cDNA probe.

For quantitative reverse transcription-PCR (RT-PCR), cDNA was synthesized using Moloney murine leukemia virus (M-MuLV) reverse transcriptase with random primers. Real-time PCR was performed with SYBR green PCR mix (Applied Biosystems). The PCR cycling conditions were as follows: 40 cycles of 30 s at 95°C, 30 s at 60°C, and 30 s at 72°C. β-Actin was used for normalization. Error bars represent standard deviations ($n = 3$). PDK expression under attached conditions was set as 1.

The primers used for the four PDKs, ERRγ, and β-actin were the following (5): PDK1, forward, 5′-CTATGAAAATGCTAGGCGTCTGT-3′, and reverse, 5′-AACCACTTGTATTGGCTGTCC-3′; PDK2, forward, 5′-AGGACACCTACGGCGATGA-3′, and reverse, 5′-TGCCGATGTGTTTGGGATGG-3′; PDK3, forward, 5′-GCCAAAGCGCCAGACAAAC-3′, and reverse, 5′-CAACTGTCGCTCTCATTGAGT-3′; PDK4, forward, 5′-TTATACATACTCCACTGCACCA-3′, and reverse, 5′-ATAGACTCAGAAGACAAAGCCT-3′; ERRγ, forward, 5′-TCTTGCTAATTCAGACTCCAT-3′, and reverse 5′-GCAGTGTCATCAGCATCTTG-3′; β-actin, forward, 5′-AGAAAATCTGGCACCACACC-3′, and reverse, 5′-AGAGGCGTACAGGGATAGCA-3′.

**Western blotting.** Cells were lysed in denaturing lysis buffer (50 mM Tris [pH 7.5], 1 mM EDTA, 1% SDS, adding dithiothreitol [DTT] to 20 mM before use), followed by SDS-PAGE and immunoblotting. The following antibodies were used for Western blotting: rabbit anti-PDK1 antibody (Cell Signaling), rabbit anti-PDK2 antibody (Epitomics), rabbit anti-PDK4 antibody (Abgent), rabbit anti-LDHA antibody (Cell Signaling), mouse anti-Flag antibody (Sigma), and mouse antitubulin antibody (Sigma).

**Luciferase reporter assay.** MCF10A cells were transfected with the PDK4 promoter luciferase reporter, simian virus 40-driven *Renilla* reporter, and ERRγ expression or control vector plasmid and harvested for a luciferase assay after 24 h of incubation. Luciferase activities were determined using the dual luciferase reporter assay system (Promega, Madison, WI). *Renilla* luciferase was used as a reference to normalize transfection efficiencies in all experiments.

**ChIP assay.** Cells were cross-linked with 1% formaldehyde for 10 min. The reaction was stopped by the addition of glycine. Cross-linked cells were washed in 1× phosphate-buffered saline and collected. Cell pellets were washed in washing buffer (0.25% Triton X-100, 10 mM EDTA, 0.5 mM EGTA, 10 mM Tris [pH 8.0]), resuspended in sonication buffer (1 mM EDTA, 0.5 mM EGTA, 10 mM Tris [pH 8.0]), mixed with glass beads,

and subjected to sonication. The sonicated samples were diluted in chromatin immunoprecipitation (ChIP) buffer (0.01% sodium dodecyl sulfate, 1.0% Triton X-100, 1.0 mM EDTA, 20 mM Tris [pH 8.1], 150 mM NaCl) and incubated with specific antibodies and protein A slurry (Invitrogen). The immunoprecipitates were subjected to a series of washing steps to remove nonspecific binding. After reverse cross-linking, the DNA samples were purified and then analyzed by real-time quantitative PCR. Final results represent the percentage of input chromatin, and error bars indicate standard deviations from triplicate experiments.

**Measurement of PDH activity.** PDH activity was measured using the Dipstick assay kit from MitoSciences (MSP30). Cells were lysed in the 10× sample buffer provided with the kit, followed by centrifugation and measurement of protein concentration using the bicinchoninic acid (BCA) kit. One milligram of protein lysate was loaded, and PDH activity was measured following the Dipstick assay protocol.

**Depletion of PDKs and ERRγ by retroviral and lentiviral shRNA transduction.** PDK4 and PDK1 genes were depleted in MCF10A and MDA-MB-231 cells, respectively, by retroviral transduction using the MSCV-LMP vector (OpenBiosystems). The RNA interference (RNAi) Oligo Retriever program was used to generate hairpin PCR primers: for PDK4, two different short hairpin RNA (shRNA) targets, 5′-ACCAACG CCTGTGATGGATAAT-3′ and 5′-TATTTATCATCTCCAGAATTAA-3′; for PDK1, 5′-TTCTACATGAGTCGCATTTCAA-3′ (reference 27); for PDK2, 5′-GCGCCTGCCTGTCTACAACAAG-3′. ERRγ was depleted in MCF10A cells by lentiviral transduction using a pGIPz vector (OpenBiosystems). The shRNA target used was 5′-CAGTGGGAGCTACAGTT CA-3′.

**Trypan blue exclusion assay and caspase 3/7 activity assay.** Cell viability was determined using 0.4% trypan blue dye in a hemacytometer. Dead cells were stained blue. The caspase 3/7 assay was performed using Caspase 3/7 Glo assay kit from Promega. Cells were lysed in hypertonic buffer (HTB; 10 mM HEPES [pH 7.9 at 4°C], 1.5 mM $MgCl_2$, 10 mM KCl, adding 0.2 mM phenylmethylsulfonyl fluoride [PMSF]; 0.5 M DTT freshly added before use). The protein concentration of samples was measured using the BCA kit. Aliquots of 75 to 100 μg of protein were loaded in each of the 96-well microplates, and the caspase 3/7 assay was performed following the manufacturer's instructions.

**Annexin V/7-AAD analysis.** Annexin V preferentially binds to phosphatidylserine (PS). Under normal physiologic conditions, PS is predominantly located in the inner side of the plasma membrane. Upon initiation of apoptosis, PS is translocated to the outer surface of the membrane and can be detected by fluorescently labeled annexin V. In early stage apoptosis, the plasma membrane remains intact and excludes viability dyes, such as 7-aminoactinomycin D (7-AAD; BD Pharmingen), and so early apoptotic cells will only stain with annexin V (no or little 7-AAD). In late-stage apoptosis, the integrity of the cell membrane is lost and annexin can bind PS, whereas 7-AAD can stain DNA. The late-stage apoptotic cells are annexin V and 7-AAD double positive. A total of $1 \times 10^5$ cells were washed twice with PBS, followed by staining with phycoerythrin (PE)-annexin V and 7-AAD for 15 min at room temperature, following the manufacturer's instruction. Cells were analyzed within an hour using Becton Dickson's Facsort apparatus. CellQuest software was used to analyze the data as an [FL2H, FL3H] log-scale two-dimensional diagram.

**Measurement of oxygen consumption rate.** Oxygen consumption was measured using 96-well oxygen biosensor plates from BD Biosciences. One million cells from attached and suspension cultures were loaded into a 96-well BD biosensor plate to measure the oxygen consumption rate for 2 h at 10-min intervals. Fluorescence was measured using an excitation wavelength of 590 nm and emission wavelength of 630 nm (Ex/Em of 590/630).

**Measurement of ATP levels.** ATP levels were measured using Promega's Cell Titer Glo assay kit. One million living cells from attached and suspension cultures were loaded into a 96-well plate, and ATP was measured using a luminometer.

**Measurement of intracellular ROS.** Intracellular ROS was measured using the Amplex red hydrogen peroxide/peroxidase kit from Invitrogen. Cells were grown under attached and suspension conditions followed by lysis using HTB (10 mM HEPES [pH 7.9 at 4°C], 0.5 mM $MgCl_2$, 10 mM KCl, adding 0.2 mM PMSF). An equal amount of protein was loaded into a 96-well plate, and ROS levels were measured as per the instructions for the Amplex red assay kit. Fluorescence was measured using an Ex/Em of 590/630.

**Measurement of mitochondrial ROS (superoxide) using MitoSOX Red.** Cells were grown in petri dishes coated with polyHema. After 24 h of incubation, the suspended cells were collected by centrifugation at 1,000 rpm for 3 min, followed by a brief wash with PBS. A final concentration of 5 μM MitoSOX Red (Life Technologies) was added to cells according to the manufacturer's recommendation. Cells were incubated with MitoSOX for 10 min at 37°C. After incubation, cells were washed twice with PBS and suspended at a density of $0.5 \times 10^6$ cells/400 μl PBS. Mitochondrial superoxide was measured by flow cytometry using a FACSCalibur apparatus (BD Bioscience, San Jose, CA). MitoSOX Red was excited by a laser at 488 nm. The data were collected as forward and side scatter based on 585/42 nm (FL2) and 670LP (FL3) channels.

**Measurement of intracellular lactate.** Intracellular lactate was measured using the lactate assay kit from Biovision. As per the manufacturer's protocol, 1 million cells were assayed to measure lactate levels, with Ex/Em of 590/630.

**Experimental metastasis assay in mice.** Four- to 5-week-old female SCID/Beige mice were purchased from Harlan. Control and shPDK1 MDA-MB-231 cells were cultured under adherent conditions. After trypsinization, 2 million cells were resuspended in 200 μl PBS and injected via the intravenous route into a total of six mice for each group. Forty days postinjection, lungs were harvested from the mice after euthanasia. All procedures were approved by the University of Florida IACUC.

**Tissue sectioning and H&E staining.** Tissue sectioning, processing, and hematoxylin and eosin (H&E) staining were performed by the Cell and Tissue Analysis Core (CTAC) facility at the University of Florida. Lung tissues were paraffin embedded and sectioned at 5 μm. For H&E staining, deparaffinization was conducted, followed by staining with hematoxylin and eosin.

**Statistics.** Student's two-tailed *t* test was used to calculate *P* values.

## RESULTS

**Induction of PDK4 by matrix detachment.** Pyruvate, the terminal product of glycolysis, is primarily converted to acetyl-CoA in the mitochondria by the PDH complex in normal cells, or to lactate in the cytoplasm by lactate dehydrogenase (LDH) in cancer cells. Thus, the fate of pyruvate represents a nodal point where glucose metabolism of normal and cancer cells differs fundamentally. As normal and cancer cells also show differential sensitivity to anoikis, we decided to investigate the relationship between glucose metabolism and anoikis by examining potential regulation of PDH and LDH during cell detachment.

PDH is a multisubunit enzymatic complex, and its activity is tightly regulated by phosphorylation on the E1α subunit by PDKs 1 to 4 (28). We first compared the RNA levels of all 4 PDK isoenzymes by quantitative RT-PCR in primary HMECs before and after matrix detachment. PDK4, which was barely detectable in adherent cells, was dramatically induced when HMECs were detached from matrix (Fig. 1A). This induction occurred 24 h after cell detachment (Fig. 1B). Other PDKs exhibited little or modest changes (Fig. 1A).

We then examined expression of PDKs in the MCF10A human mammary epithelial cell line. Transcripts of PDK4 were also strongly upregulated in suspended MCF10A cells (Fig. 1C). Significant upregulation of PDK4 was first observed 12 h after cell

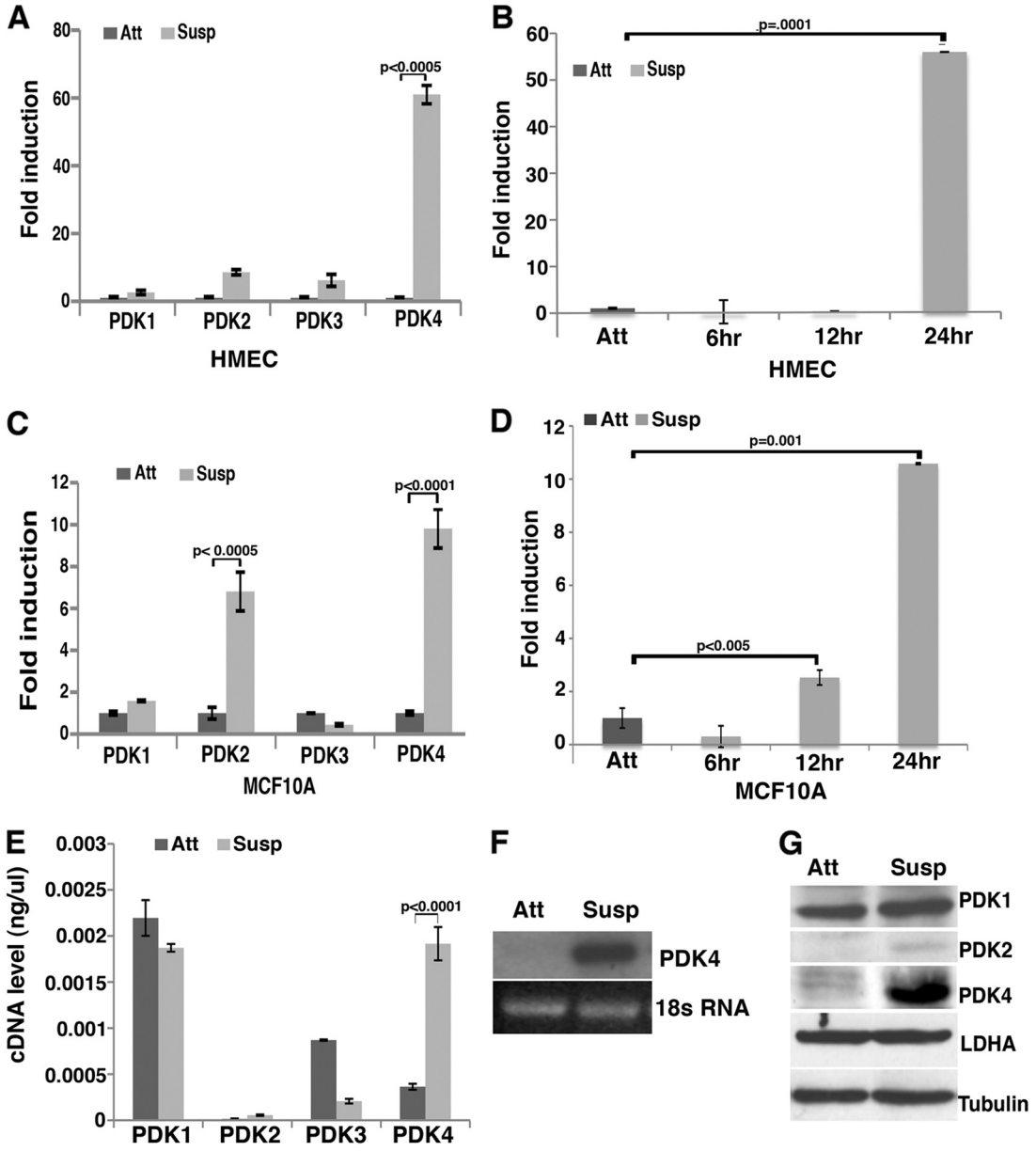


**FIG 1** Matrix detachment upregulates PDK4 in mammary epithelial cells. (A) Quantitative RT-PCR measurement of individual PDKs in HMEC under attached (Att) and suspended (Susp) conditions. (B) Time course of PDK4 induction in HMEC under suspension. (C) Quantitative RT-PCR analysis of expression of PDKs in MCF10A cells. (D) Induction of PDK4 in suspended MCF10A cells at the indicated time points. (E) Quantitative RT-PCR analysis of absolute levels of PDKs in attached and suspended MCF10A cells. cDNA plasmids of each PDK were used as references. (F) Northern blotting of PDK4 in attached and suspended MCF10A cells. (G) Immunoblotting of PDKs, LDHA, and tubulin in attached and suspended MCF10A cells.

detachment and peaked by 24 h (Fig. 1D). PDK1 and PDK3 did not show notable changes. We measured the absolute transcript quantity of each PDK in MCF10A cells. Although PDK2 was also induced by detachment, its abundance in suspended MCF10A cells was negligible (Fig. 1E). Indeed, PDK1 and PDK4 were found to be the predominant PDKs in suspended MCF10A cells (Fig. 1E).

Robust induction of PDK4 by detachment of MCF10A cells was further verified by Northern blotting. PDK4 RNA was absent in adherent MCF10A cells but became readily detected in suspended cells (Fig. 1F). Consistent with RNA expression, PDK4 protein was not detected in adherent cells but was markedly induced following cell detachment (Fig. 1G). Western blotting also showed that PDK1 protein was present in MCF10A but did not increase significantly under suspension conditions, and PDK2 was not detectable regardless of the cell-matrix contact status (Fig. 1G). Furthermore, the protein levels of LDHA did not change when cells lost adhesion to ECM. Together, these observations demonstrate that PDK4 is strongly induced in human mammary epithelial cells by matrix detachment.

**Upregulation of PDK4 antagonizes anoikis.** Matrix detachment has a profound effect on cellular metabolism and causes changes in gene expression (31). To determine whether upregulation of PDK4 might be simply a consequence of detachment or actively influence detachment-induced cell death, we depleted

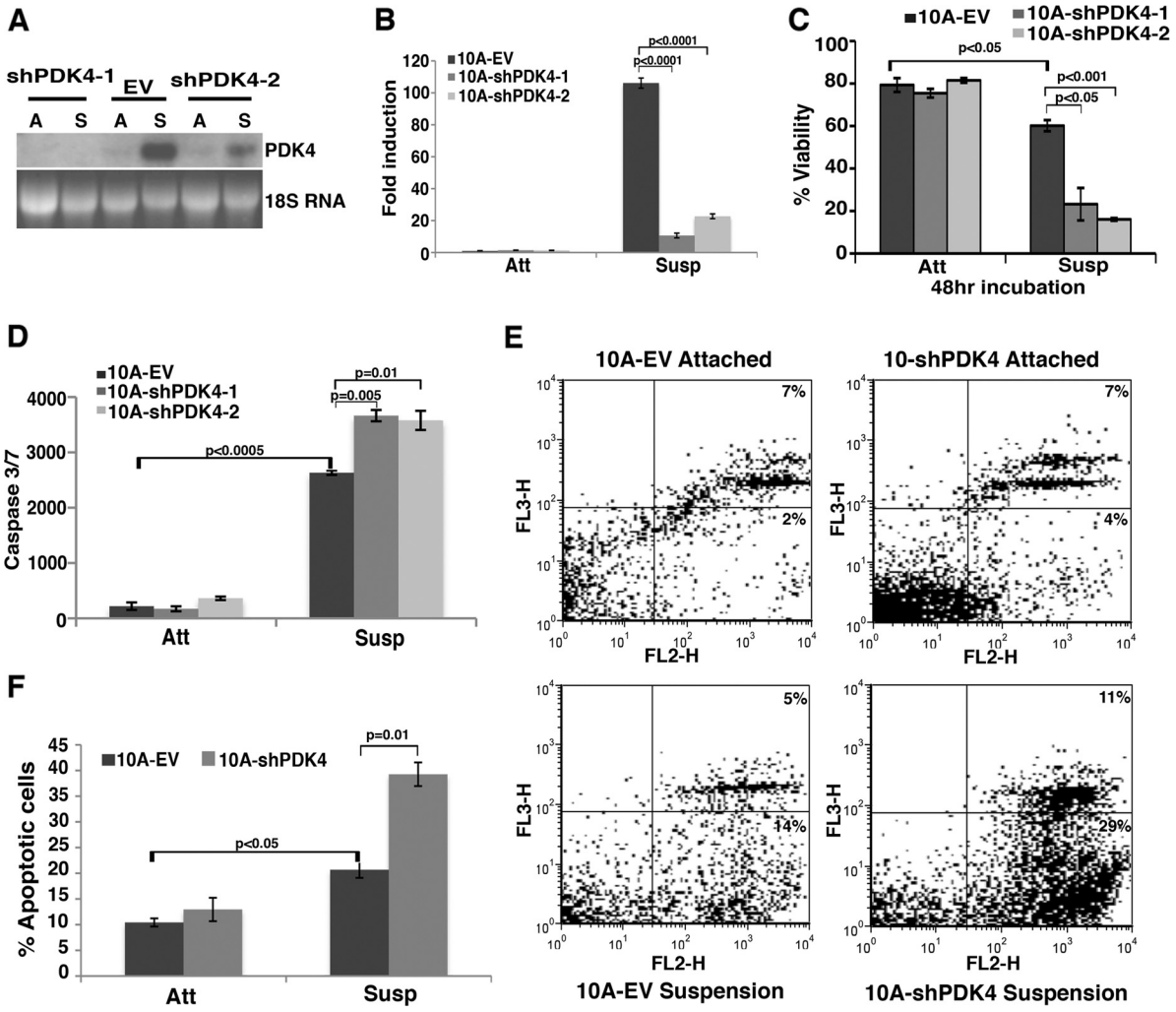


**FIG 2** Depletion of PDK4 in MCF10A cells enhances anoikis. MCF10A cells were transduced with a retroviral vector (EV) or two independent shRNAs targeting PDK4 (shPDK4) and cultured under attached (Att) and suspended (Susp) conditions for 24 h (unless otherwise indicated). Error bars represent standard deviations. (A) Northern blotting of PDK4 depletion in MCF10A cells under attached (A) and suspended (S) conditions. 18S rRNA was used as a loading control. (B) Quantitative determination of PDK4 knockdown efficiency in MCF10A cells under attached and suspended conditions. The RNA level of PDK4 in suspended MCF10A cells was set as 100. (C) Trypan blue exclusion assay of cell viability in control and PDK4-depleted MCF10A cells under attached and suspended (for 48 h) conditions. (D) Measurement of caspase 3/7 activity in control and PDK4-depleted MCF10A cells. (E) Fluorescence-activated cell sorting analysis of annexin V/7-AAD staining in control and PDK4-depleted MCF10A cells. The *x* axes show annexin V staining, and *y* axes show 7-AAD staining. (F) Statistics of total apoptotic cells based on the annexin V/7-AAD analysis.

PDK4 in MCF10A cells by RNAi and examined its effect on anoikis. Efficient knockdown of PDK4 by two independent retroviral shRNAs was verified in attached and suspended MCF10A cells by both Northern blotting and quantitative RT-PCR (Fig. 2A and B, respectively). Under adherent culture conditions, no difference in cell death (based on trypan blue exclusion) was observed between control and PDK4-depleted cells (Fig. 2C), which is consistent with a lack of PDK4 expression in adherent MCF10A cells. However, under suspension culture, PDK4-depleted cells showed significantly increased cell death compared to control cells (Fig. 2C).

To validate that increased cell death was at least in part attributed to apoptosis, we first conducted a caspase 3/7 activity assay (Fig. 2D). When cells were attached to matrix, little caspase activity was detected in either control or PDK4-depleted MCF10A cells. Upon detachment, cells underwent anoikis, and the caspase activity significantly increased in control cells (Fig. 2D). The suspended PDK4-depleted cells displayed even higher caspase activity than the suspended control cells (Fig. 2D), indicating increased apoptosis. We next performed PE-annexin V/7-AAD analysis (Fig. 2E and F). Under attached conditions, no significant difference in apoptosis was detected between control and PDK4-depleted MCF10A cells. Upon cell detachment, an increase in apoptotic cells was observed in both cell groups. Compared to control cells, PDK4-depleted cells exhibited elevated early-stage (29% versus 14%) and late-stage (11% versus 5%) apoptosis when detached from matrix (Fig. 2E). As a control, we depleted PDK2 and investigated its influence on anoikis. Although PDK2 was upregulated upon matrix detachment (Fig. 1C), it was expressed at relatively low levels in MCF10A cells (Fig. 1E), and depletion of PDK2 did not cause significant changes in anoikis (data not shown). Therefore, upregulation of PDK4 in response to matrix detach-

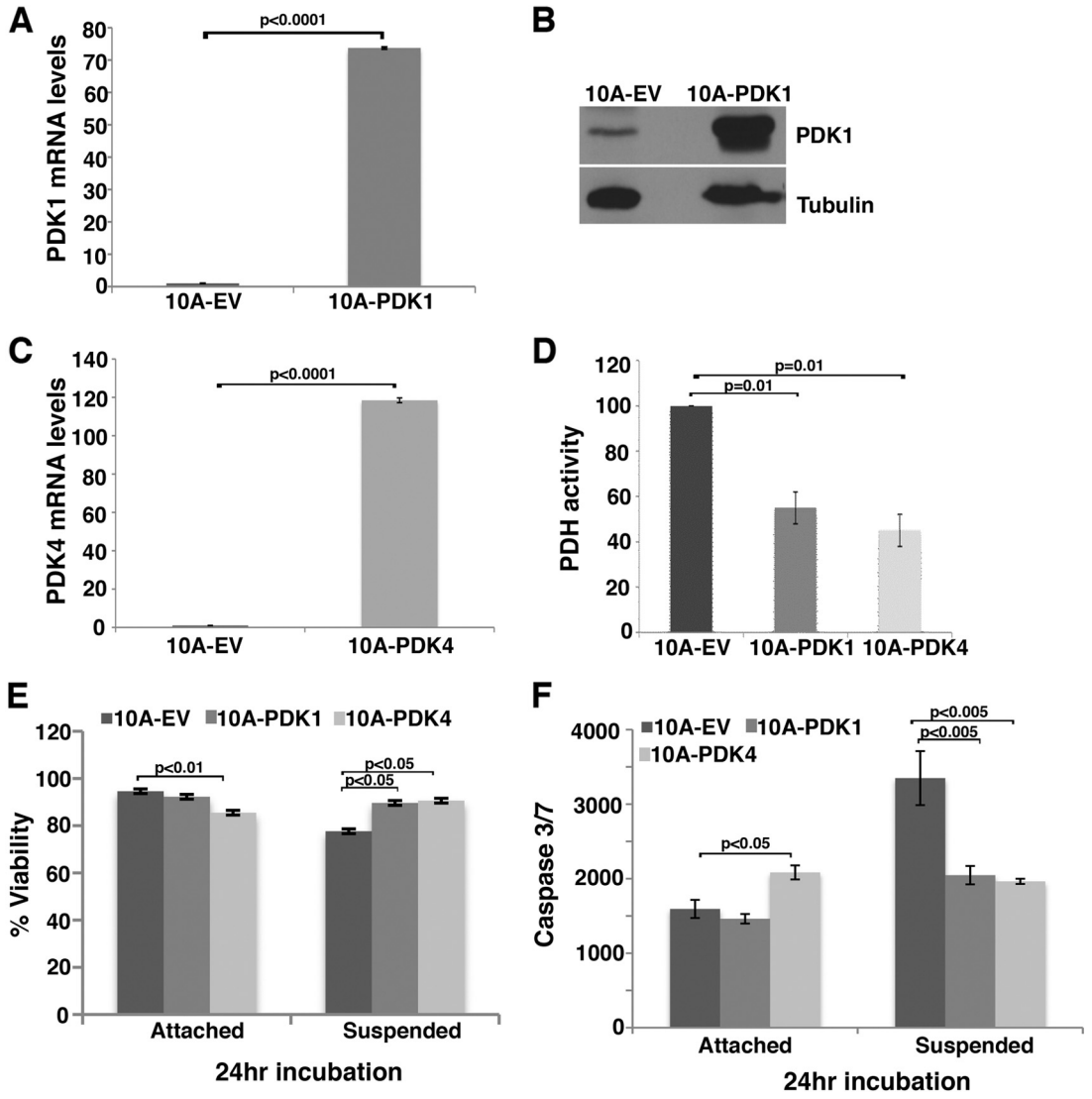


**FIG 3** Overexpression of PDK1 or PDK4 blunts anoikis. MCF10A cells were transduced with control (EV) or PDK1- or PDK4-expressing lentiviruses and subjected to anoikis analysis (24 h in suspension). (A and B) Quantitative RT-PCR (A) and Western blotting assay (B) results to verify overexpression of PDK1 in attached MCF10A cells. (C) Quantitative RT-PCR validation of PDK4 overexpression in attached MCF10A cells. (D) PDH activities in PDK1- and PDK4-overexpressing MCF10A cells under attached conditions. PDH activity in control cells was set as 100. (E) Trypan blue cell viability assay of control or PDK1- or PDK4-overexpressing cells under attached and suspended conditions. (F) Caspase 3/7 activity assay in control or PDK1- or PDK4-overexpressing cells under attached and suspended conditions.

ment protected mammary epithelial cells from anoikis and prolonged their survival specifically in suspension.

**Overexpression of PDK1 or PDK4 protects cells from anoikis.** Following detachment, cells induce PDK4 to extend their viability. However, this transcriptional process takes approximately 24 h (Fig. 1B and D), and during this period a substantial fraction of cells die in suspension. We reasoned that preexpression of PDK4 in cells before detachment might blunt a cell's sensitivity to anoikis. Because of the functional similarities among different PDK members, we generated lentiviral expression vectors for both PDK1 and PDK4 and infected MCF10A mammary cells. Transduced cells expressed high levels of PDK1 or PDK4 (Fig. 3A to C), which led to decreased PDH activity (Fig. 3D). Under adherent conditions, overexpression of PDK1 did not show any effect on cell viability, but overexpression of PDK4 caused slight yet significant cell death (Fig. 3E). Importantly, when cells were placed in suspension, overexpression of either PDK1 or PDK4 significantly blocked cell death (Fig. 3E) and detachment-induced caspase activation (Fig. 3F). These results suggest that preexisting high levels of PDKs in cells confer anoikis resistance and help cells survive in suspension.

**Activation of PDH sensitizes cells to anoikis.** We were interested in dissecting the mechanism by which PDKs promote cell survival in suspension. PDKs are known to control glucose metabolism by phosphorylating and inactivating PDH, thereby reducing glucose oxidation. PDH activity was indeed reduced in MCF10A cells overexpressing PDK1 or PDK4 (Fig. 3D). Upregulation of PDK4 in suspended cells was expected to inhibit PDH. This was confirmed by direct determination of PDH activity in MCF10A cells under adherent and suspension culture conditions.

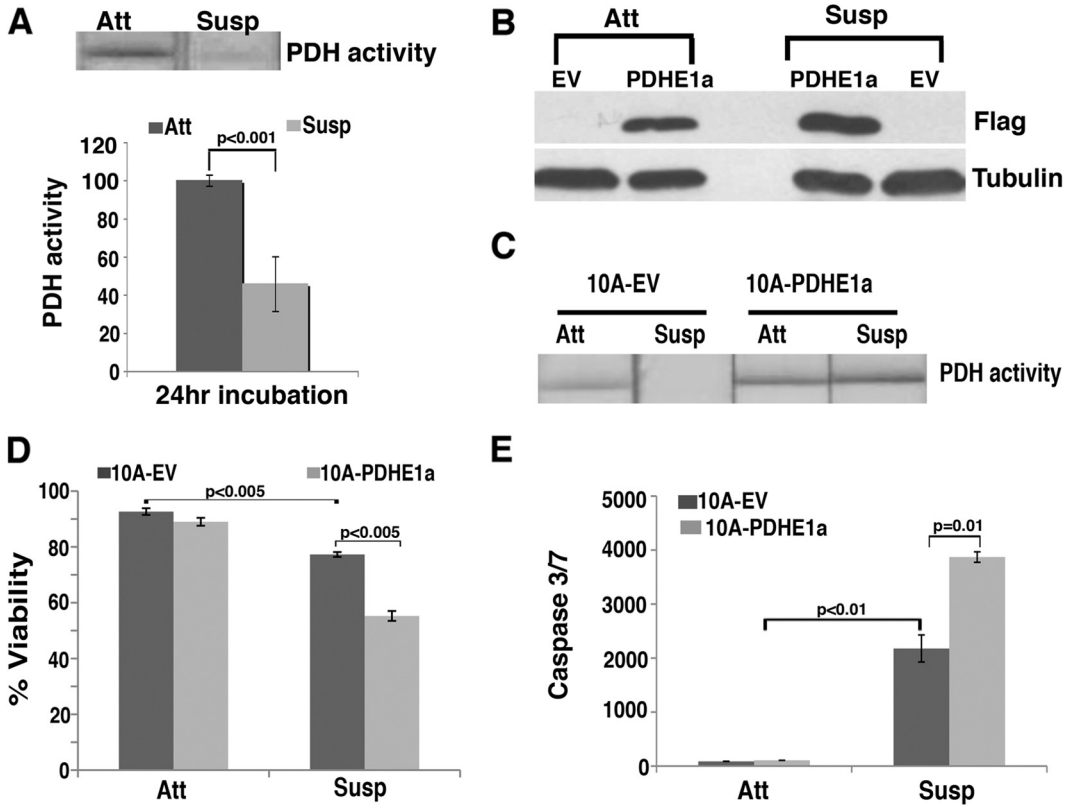


**FIG 4** Activation of PDH enhances anoikis in MCF10A cells. MCF10A cells were transduced with a lentiviral vector (EV) or lentivirus expressing a constitutively active form of PDHE1α with a carboxyl-terminal Flag tag (PDHE1a). Error bars represent standard deviations ($n = 3$). (A) Measurement of PDH activity in MCF10A cells under attached (Att) and suspended (Susp) conditions. (B) Immunoblotting of exogenous PDHE1α expression with anti-Flag antibodies. (C) Measurement of PDH activity in control and PDHE1α-expressing cells cultured under attached and suspended conditions. (D) Trypan blue exclusion assay for cell viability in control and PDHE1α-expressing MCF10A cells under attached and suspended conditions. (E) Caspase 3/7 activity assay in control and PDHE1α-expressing MCF10A cells under attached and suspended conditions.

The PDH activity was significantly downregulated in matrix-detached cells compared with attached cells (Fig. 4A).

If PDK4 modulated anoikis through regulation of PDH, manipulation of PDH activity would affect cell viability as well. PDKs inactivate PDH by phosphorylating the E1α subunit at serine residues 232, 293, and 300 (28). We constructed a constitutively active form of PDHE1α by replacing these serines with alanines and introduced it into MCF10A cells by lentiviral transduction. Expression of the exogenous PDHE1α was confirmed by Western blotting (Fig. 4B). Unlike the control cells, which reduced PDH activity in suspension, cells transduced with active PDHE1α displayed increased PDH activity under both attached and suspended conditions (Fig. 4C). When cells were subjected to detachment, the constitutively active PDHE1α significantly enhanced cell death (Fig. 4D) and apoptosis (Fig. 4E). No notable cell death or apoptosis by activated PDHE1α was observed in cells under attached conditions. Therefore, similar to depletion of PDK4, activation of PDH sensitizes cells to anoikis. Taken together, detachment from ECM in mammary epithelial cells potently activates PDK4 expression and consequently decreases PDH activity, leading to increased cell survival. Depletion of PDK4 or activation of PDH enhances anoikis.

**Depletion of PDK4 increases mitochondrial oxidation and ROS production.** It was unclear how the PDK4-PDH axis affects a cell's sensitivity to anoikis. PDH critically controls the entry of pyruvate into the mitochondrial TCA cycle. Decreased PDH activity should lead to a reduced flux of pyruvate into acetyl-CoA and mitochondrial oxidation. The above results led us to infer that glucose metabolism, in particular mitochondrial oxidation of pyruvate, sensitizes cells to anoikis. In fact, mitochondria are not only the energy center but also play a pivotal role in the regulation of cell death. Mitochondria are the major endogenous source of ROS, which are by-products of oxidative metabolism. Therefore, we hypothesized that depletion of PDK4 or increased PDH activity in matrix-detached cells would lead to increased mitochondrial oxidative metabolism and consequently elevated ROS levels to enhance anoikis.

To test this model, we measured PDH activity in PDK4-depleted MCF10A cells under attached and suspended conditions. Matrix detachment downregulated PDH activity in control cells, and knockdown of PDK4 increased PDH activity in suspended cells (Fig. 5A). Increased PDH activity should increase mitochondrial oxidation of glucose and oxygen consumption. To verify these metabolic changes, we determined the oxygen consumption rate (OCR) in PDK4-depleted cells. Under adherent conditions there was no significant difference in OCR between control and PDK4-depleted MCF10A cells (Fig. 5B). Upon detachment, control cells strongly decreased $O_2$ consumption (Fig. 5B), which was consistent with increased PDK4 expression and reduced PDH activity during the process. The suspended PDK4-depleted cells

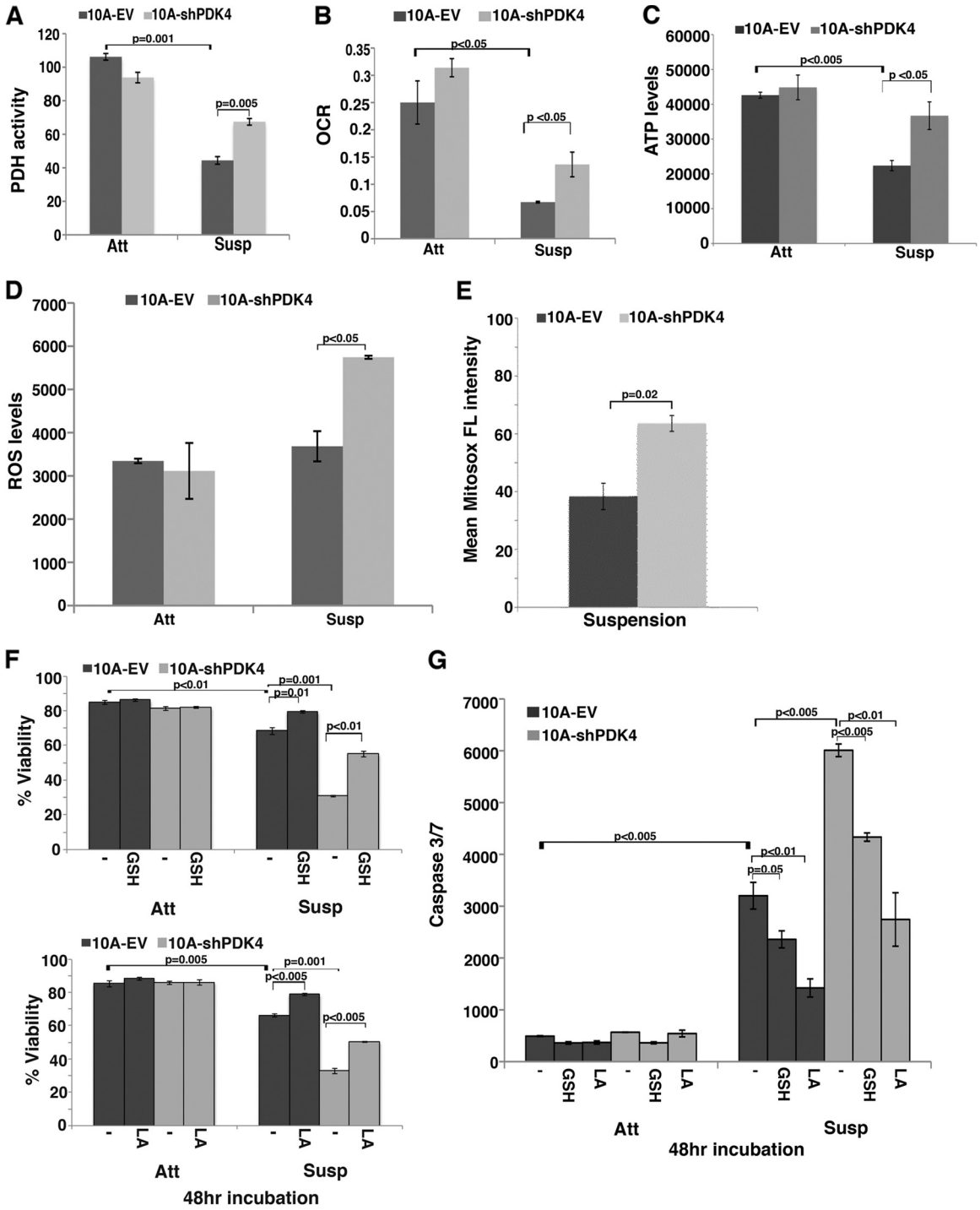


**FIG 5** Knockdown of PDK4 increases mitochondrial respiration and ROS levels in suspended MCF10A cells. Empty vector (EV) or PDK4 shRNA (shPDK4)-transduced MCF10A cells were cultured under attached (Att) and suspended (Susp) conditions. Error bars represent standard deviations ($n = 3$). (A) Measurement of PDH activity. (B) Oxygen consumption rate (OCR). (C) ATP levels. (D) Overall ROS levels in control and PDK4-depleted cells under attached and suspension (for 24 h) conditions. (E) Mitochondrial ROS detected by using MitoSOX Red in control and PDK4-depleted cells under suspension (for 24 h) conditions. (F and G) Cell viability (F) and caspase 3/7 activity (G) in cells untreated (-) or treated with 2.5 mM GSH or 100 μM LA under attached and suspension (for 48 h) conditions.

showed significantly higher OCR than the suspended control cells (Fig. 5B). In agreement with a previous study that cell detachment caused ATP deficiency (31), overall ATP levels in the control cells decreased upon matrix detachment (Fig. 5C). Under suspension conditions, PDK4-depleted cells produced significantly more ATP than the control cells (Fig. 5C). Therefore, depletion of PDK4 rescued ATP deficiency caused by matrix detachment. As PDK4-depleted cells are more sensitive to anoikis, this result implies that

ATP deficiency may not be the primary cause of cell death in suspension. These data suggest that depletion of PDK4 partially restores mitochondrial oxidation specifically in suspended mammary epithelial cells.

Increased mitochondrial oxidative metabolism is expected to generate more ROS. We determined ROS levels in control and PDK4-depleted cells under adherent and suspension culture conditions. Control cells did not significantly increase overall ROS levels when detached from matrix (Fig. 5D). Consistent with increased mitochondrial activity, PDK4-depleted cells accumulated significantly more overall ROS and mitochondrial ROS than control cells under suspension culture (Fig. 5D and E).

Because matrix detachment accompanies an increase in proapoptotic BH3 factors (11), suspended cells may display heightened sensitivity to ROS. To validate that ROS contributes to anoikis, we treated cells with antioxidants, including the reduced form of glutathione (GSH) and α-lipoic acid (LA) to scavenge the intracellular ROS. GSH is one of the most prevalent intracellular reducing agents to maintain redox homeostasis. GSH reacts with ROS to form GSSG (oxidized form). LA is a clinically used free radical scavenger that is readily converted into the reduced form by intracellular antioxidant enzymes, such as glutathione reductase. The reduced form of LA has potent antioxidant activity. Antioxidant treatment had little effect on cell death or apoptosis in adherent control or PDK4-depleted cells (Fig. 5F and G). Suspended control MCF10A cells underwent anoikis, which was attenuated by treatment with antioxidants (Fig. 5F and G). These results imply that cells become hypersensitive to ROS in the absence of matrix attachment. Consistent with higher intracellular ROS levels in suspension, PDK4-depleted cells displayed elevated anoikis compared to control cells, which was also substantially suppressed by antioxidants (Fig. 5F and G). Together, these findings suggest that upon detachment from matrix, cells upregulate PDK4 to attenuate PDH activity and mitochondrial oxidation of pyruvate. This metabolic shift reduces ROS production and oxidative stress, rendering cells more resistant to anoikis.

**Estrogen-related receptor gamma activates PDK4 in response to cell detachment.** Due to the critical role of PDK4 in matrix detachment-induced metabolic shift and anoikis, it is important to understand the transcriptional mechanism underlying the activation of PDK4 following cell detachment. PDK4 was previously identified as a direct target of the ERRs (2, 7, 36, 37). ERRs are orphan nuclear receptors and play a key role in energy metabolism by regulating mitochondrial biogenesis and fatty acid oxidation (10). There are three ERR members. ERRα and ERRγ are expressed in metabolically active tissues, whereas ERRβ is largely restricted to embryonic cells.

We first examined expression of ERRs in MCF10A cells under attached and suspended culture conditions. ERRα did not display significant changes (data not shown). In contrast, ERRγ was potently induced by cell detachment (Fig. 6A). We then carried out ChIP analysis to verify if ERRγ might directly bind to the PDK4 gene. We generated cells stably expressing Flag-tagged ERRγ, and the ChIP assay with an anti-Flag antibody confirmed the binding of ERRγ to the proximal promoter of PDK4 (Fig. 6B). Next, using a luciferase reporter driven by the PDK4 promoter, we observed strong activation of the reporter by exogenous ERRγ in transiently transfected MCF10A cells (Fig. 6C). Finally, to test if ERRγ was responsible for induction of PDK4 by cell detachment, we efficiently depleted ERRγ with a lentiviral shRNA (Fig. 6D). In ERRγ-depleted cells, induction of PDK4 by matrix detachment was substantially reduced (Fig. 6D), suggesting that ERRγ is a major activator of PDK4 in suspended MCF10A cells. PDK1 expression was not affected by depletion of ERRγ (data not shown).

Because ERRγ is essential for activating PDK4 in response to matrix detachment, it was expected that depletion of ERRγ also enhances anoikis. We therefore compared cell death in ERRγ-depleted MCF10A cells under adherent and suspension conditions. Depletion of ERRγ had no effect on cell viability in adherent cells, but ERRγ-depleted cells in suspension exhibited increased cell death and apoptosis compared to control cells in suspension (Fig. 6E and F). Therefore, we conclude that in untransformed mammary epithelial cells, matrix detachment induces ERRγ, which in turn activates transcription of PDK4 and consequently results in decreased glucose oxidation and extended cell survival in suspension (Fig. 6G).

**PDK4 is overexpressed in a subset of human cancers and contributes to anoikis resistance in cancer cells.** In untransformed cells, depletion and overexpression of PDK4 enhances and attenuates a cell's sensitivity to anoikis, respectively. While untransformed mammary epithelial cells activate the ERRγ-PDK4 pathway to attenuate mitochondrial respiration for survival in suspension, cancer cells constitutively display increased glycolysis and decreased glucose oxidation even under attached conditions. Therefore, cancer cells are expected to possess a survival advantage when detached from matrix. Indeed, cancer cells are resistant to anoikis. Given the important role of PDK4 in modulating anoikis sensitivity in normal cells, we asked whether PDK4 might contribute to anoikis resistance in cancer cells.

We surveyed human cancer cells for possible overexpression of PDK4. Microarray analysis of the NCI's panel of 60 human cancer cell lines from 9 common tumor types revealed that PDK4 is highly expressed in more than 10% of these lines, including SNB-75 (renal cancer), SKOV3 (ovarian cancer), DU-145 (prostate cancer), A549, NCI-H23, and EKVX (lung cancer), and SKMEL-5, UACC-62, and -257 (melanoma) (http://smd.stanford.edu/cgi-bin/source/sourceSearch) (30).

The high expression level of PDK4 in SKMEL-5 cells was validated by quantitative RT-PCR (Fig. 7A). Because overexpression of PDK4 in untransformed mammary cells suppresses anoikis (Fig. 3), we postulated that PDK4 in SKMEL-5 cells might regulate cell survival in suspension. We depleted PDK4 with shRNA (Fig. 7B). When placed in suspension culture, the control SKMEL-5 cells did not show any changes in cell viability; by contrast, PDK4 depletion significantly increased cell death (Fig. 7C) and caspase activity (data not shown). These results suggest that high levels of PDK4 in a subset of cancer cells may contribute to their resistance to anoikis.

**Metabolic normalization in cancer cells restores anoikis and decreases metastasis.** The Warburg effect describes a cancer cell's propensity for glycolysis instead of oxidative metabolism of glucose. Different cancer cells may exploit distinct means (including different PDKs) to achieve low glucose oxidation and anoikis resistance. To test whether altered glucose metabolism in cancer cells intrinsically confers anoikis resistance, we decided to reprogram glucose metabolism in cancer cells and examine its effect on cell viability in suspension. MDA-MB-231 triple-negative metastatic breast cancer cells are highly glycolytic even under normoxic conditions (9). The activated form of PDHE1α was ectopically introduced into MDA-MB-231 cells by lentiviral transduction

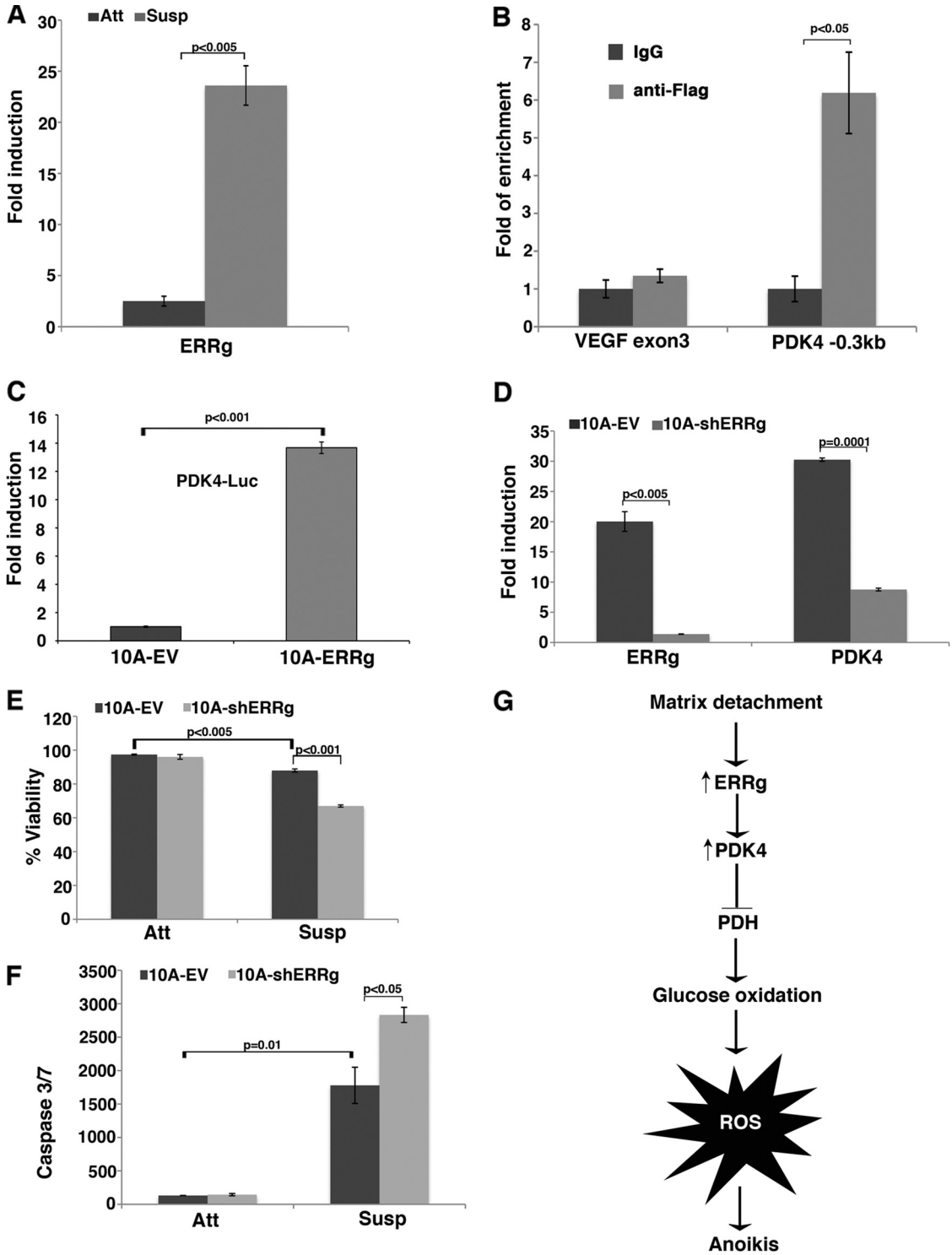


**FIG 6** ERRγ activates PDK4 in response to matrix detachment. (A) Quantitative RT-PCR analysis of ERRγ induction in MCF10A cells by matrix detachment. (B) ChIP assay of Flag-ERRγ binding to the PDK4 promoter. Control and Flag-ERRγ stable cells were subjected to ChIP with IgG and anti-Flag antibodies. Bound DNA was analyzed by quantitative PCR. Vascular endothelial growth factor (VEGF) exon 3 served as a negative control. (C) Activation of a PDK4-Luc reporter by exogenous ERRγ in transiently transfected MCF10A cells (attached). (D) Depletion of ERRγ in MCF10A cells diminished induction of endogenous PDK4 following cell detachment. MCF10A cells were transduced with a retroviral empty vector (EV) or shRNA targeting ERRγ (shERRg). Cells were plated in suspension for 24 h, and total RNA was extracted and analyzed by quantitative RT-PCR. (E) Trypan blue exclusion assay for cell viability in control and ERRγ-depleted MCF10A cells under attached and suspended conditions. (F) Caspase 3/7 activity assay in control and ERRγ-depleted MCF10A cells under attached and suspended conditions. (G) Schematic of metabolic reprogramming by activation of the ERRγ-PDK4 pathway in untransformed mammary epithelial cells following matrix detachment.

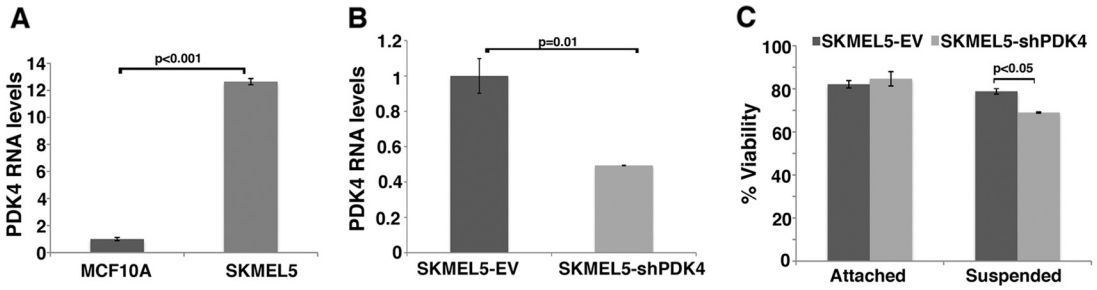


**FIG 7** PDK4 is highly expressed in SKMEL-5 cells and contributes to anoikis resistance. (A) Comparison of PDK4 levels in attached MCF10A and SKMEL-5 cells by quantitative RT-PCR. (B) Depletion of PDK4 in attached SKMEL-5 cells by shRNA. (C) Trypan blue analysis of control and PDK4-depleted SKMEL-5 cells under attached and suspended conditions.

(Fig. 8A). MDA-MB-231 cells typically exhibit very low PDH activity, which was strongly stimulated by activated PDHE1α (Fig. 8B). When subjected to suspension, the control cells completely resisted anoikis (Fig. 8C and D). PDH activation had no effect on attached cells but induced cell death and apoptosis in suspended cancer cells (Fig. 8C and D). The results suggest that low PDH activity contributes to a cancer cell's resistance to anoikis. Activation of PDH renders cancer cells susceptible to anoikis.

MDA-MB-231 cells do not express detectable PDK4 or PDK2 (based on microarray expression analysis) (30). To gain insight into why PDH activity was kept low in MDA-MB-231 cells, we measured expression of all 4 PDKs. Quantitative RT-PCR identified PDK1 as the most abundant PDK isoenzyme in MDA-MB-231 cells under both attached and suspended conditions (Fig. 9A). PDK4 was indeed also upregulated in MDA-MB-231 cells upon matrix detachment (Fig. 9B); however, its overall abundance was trivial (Fig. 9A). To further confirm that PDK1 is the primary inhibitor of PDH in these cells, we subsequently depleted PDK1 with shRNAs (Fig. 9C). Depletion of PDK1 strongly increased PDH activity in both adherent and suspended MDA-MB-231 cells (Fig. 9D), significantly decreased lactate production and increased the $O_2$ consumption rate under attached conditions (Fig. 9E and F), and increased mitochondrial ROS levels in suspension cells (Fig. 9G and H). These experiments demonstrated that depletion of PDK1 in MDA-MB-231 cancer cells shifts metabolism from aerobic glycolysis toward mitochondrial oxidation, thereby reversing the Warburg metabolic phenotype and normalizing glucose metabolism.

To further validate the effect of increased glucose oxidation by PDK1 depletion on anoikis, control and PDK1-depleted MDA-MB-231 cells were subjected to matrix detachment. Control

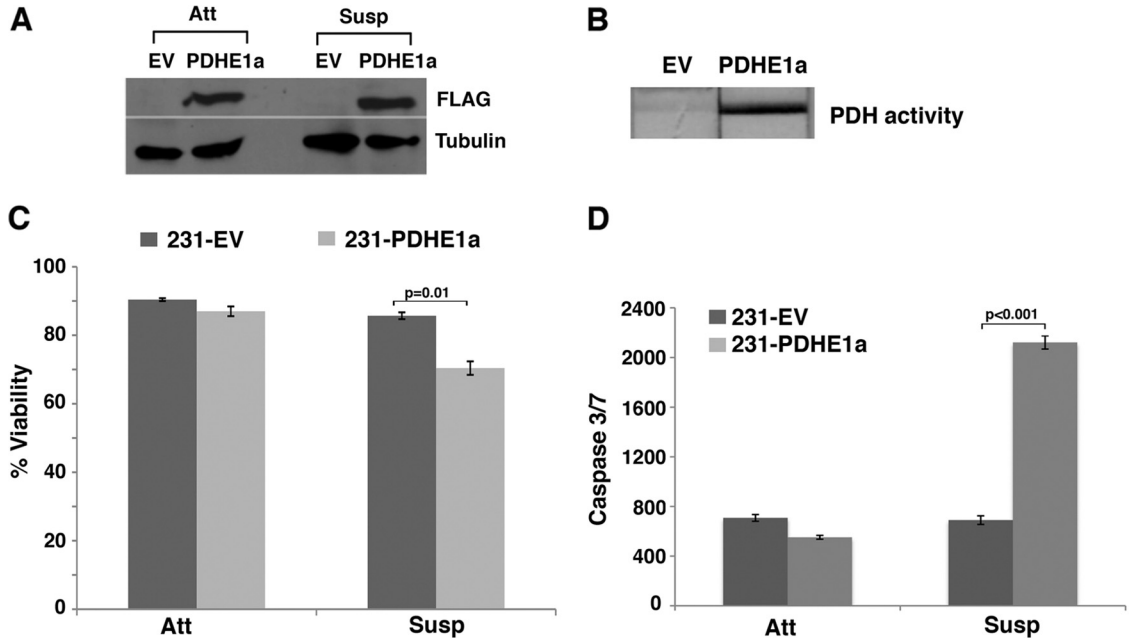


**FIG 8** Activation of PDH sensitizes MDA-MB-231 cells to anoikis. MDA-MB-231 cells were transduced with a control virus (EV) or virus expressing a constitutively active form of PDHE1α (as in Fig. 4) and subsequently subjected to matrix detachment. (A) Verification of exogenous PDHE1α expression by immunoblotting with anti-Flag antibodies. Tubulin was used as a loading control. (B) Measurement of PDH activity in control and PDHE1α-expressing cells under attached conditions. (C) Trypan blue exclusion assay for cell viability assay in control and PDH-activated MDA-MB-231 cells under attached and suspended conditions. (D) Caspase 3/7 activity assay in control and PDH-activated MDA-MB-231 cells under attached and suspended conditions. Error bars represent standard deviations ($n = 3$).

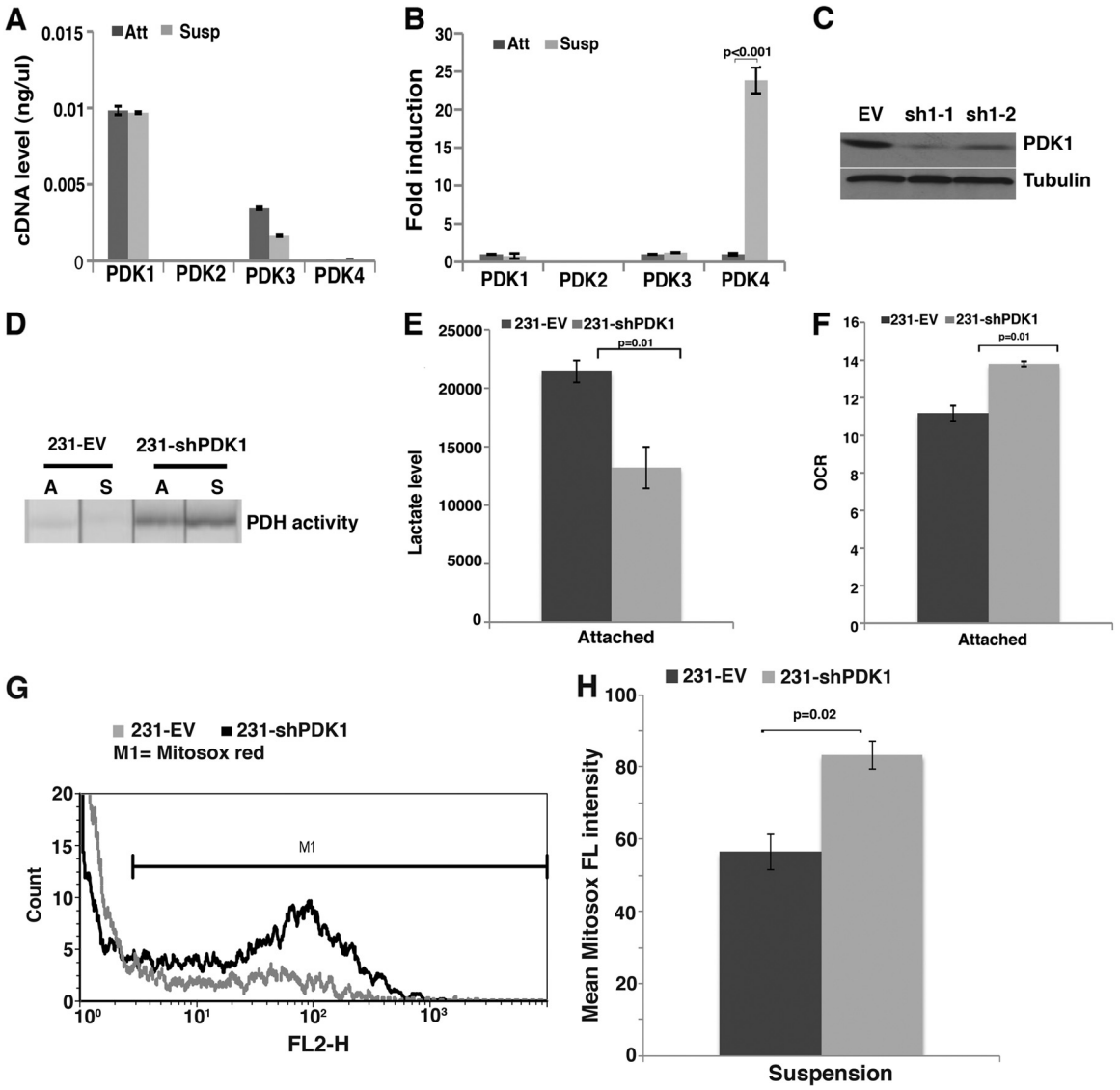


**FIG 9** Depletion of PDK1 in MDA-MB-231 cancer cells increases glucose oxidation. (A) Quantitative RT-PCR measurement of absolute levels of each PDK in MDA-MB-231 cells under attached (Att) and suspended (Susp) conditions. (B) Relative induction of PDKs in MDA-MB-231 cells grown under attached and suspended conditions. (C) Immunoblotting analysis of PDK1 depletion in MDA-MB-231 cells. MDA-MB-231 cells were infected with retrovirus of either empty vector (EV) or two independent shRNAs targeting PDK1 (shPDK1-1 and shPDK1-2). Tubulin was used as a loading control. (D) Measurement of PDH activity in control and PDK1-depleted cells under attached (A) and suspended (S) conditions. (E) Intracellular lactate levels in attached control and PDK1-depleted MDA-MB-231 cells. (F) Measurement of oxygen consumption rate (OCR) in attached control and PDK1-depleted MDA-MB-231 cells. (G) Mitochondrial ROS in control and PDK1-depleted cells under suspension (for 24 h) conditions. Representative histograms for MitoSOX Red flow cytometry are shown. The *x* axis shows the fluorescent signal intensity, and the *y* axis shows cell numbers. (H) Quantification of mean fluorescent intensity of MitoSOX Red in control and PDK1-depleted suspension cells, measured by flow cytometry (the results shown in panel G).

MDA-MB-231 cells did not show any evidence of anoikis (Fig. 10A and B). PDK1-depleted cells, even though possessing elevated PDH activity, did not display increased cell death under adherent conditions (Fig. 10A and B). Only when MDA-MB-231 cancer cells were detached from matrix did depletion of PDK1 induce cell death (Fig. 10A) and apoptosis (Fig. 10B). Together, these results suggest that normalization of glucose metabolism by depletion of PDK1 or activation of PDH is capable of restoring anoikis sensitivity in MDA-MB-231 cancer cells.

Resistance to anoikis is critical for metastasis. We examined the physiological relevance of metabolic modulation in cancer metastasis. The tail vein injection experimental metastasis assay measures the ability of cancer cells to survive in the blood circulation, extravasate, and form metastatic colonies at secondary sites. Control and PDK1-depleted MDA-MB-231 cells were cultured under adherent conditions and then trypsinized and immediately injected intravenously into immunodeficient mice. After 40 days, control MDA-MB-231 cells gave rise to about 100 tumor nodules per lung in all 6 mice analyzed (Fig. 10C and D). In contrast, PDK1-depleted cells produced 5-fold-fewer lung tumor nodules (Fig. 10C and D). Therefore, reversal of the Warburg effect by depletion of PDK1 not only sensitized metastatic cancer cells to

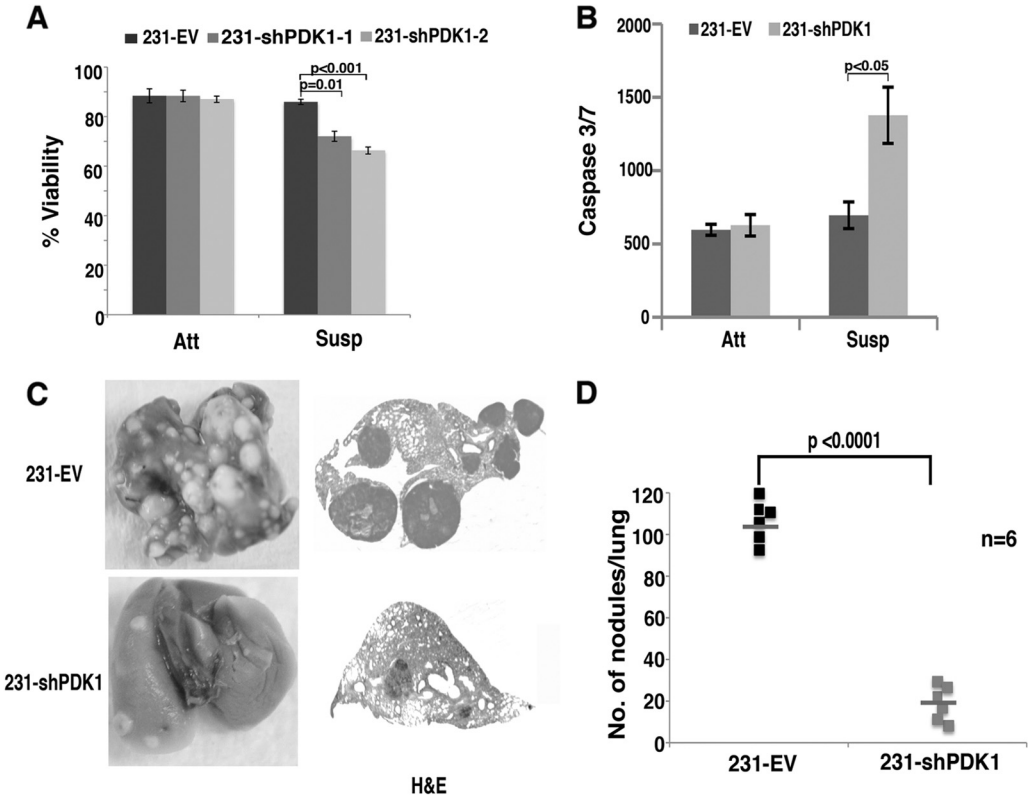


**FIG 10** Increased glucose oxidation in MDA-MB-231 cancer cells restores anoikis and decreases metastasis. (A) Trypan blue exclusion assay in control and PDK1-depleted MDA-MB-231 cells under attached (Att) and suspended (Susp) conditions (for 48 h). (B) Caspase 3/7 activity assay in control and PDK1-depleted cells under attached and suspended conditions. (C) Lung tumor nodules resulting from tail vein injection of equal numbers of control and PDK1-depleted cells followed by H&E histological analysis. (D) Statistical analysis of numbers of lung tumor nodules.

anoikis *in vitro* but also profoundly decreased their metastatic potential *in vivo*.

## DISCUSSION

The present study demonstrates that in response to cell detachment, untransformed human mammary epithelial cells markedly activate transcription of PDK4 through the nuclear receptor ERRγ. Increased expression of PDK4 inhibits PDH, thereby attenuating the conversion of glycolysis-derived pyruvate to acetyl-CoA in mitochondria and the subsequent flux into the TCA cycle. Therefore, matrix detachment profoundly inhibits glucose oxidation. Importantly, while matrix detachment causes untransformed cells to undergo apoptosis, the detachment-triggered metabolic response in turn impacts anoikis. This metabolic reprogramming diverts glucose carbons away from mitochondrial oxidative metabolism, decreases oxygen consumption and mitochondrial ROS production, and prolongs the viability of cells specifically under suspension conditions. Interruption of this metabolic adjustment by depletion of PDK4 or activation of PDH increases mitochondrial respiration and oxidative stress in suspended cells and enhances anoikis. Conversely, overexpression of PDK1 or PDK4 in untransformed cells prior to matrix detachment suppresses anoikis. These findings uncover a metabolic reprogramming mechanism by which untransformed cells manage to extend their survival in the absence of matrix contact and provide direct evidence that decreased glucose oxidation promotes anoikis resistance. During our submission of this work for publication, it was reported that matrix detachment led to global metabolic remodeling and upregulation of PDK4 in untransformed mammary cells (12). Moreover, overexpression of PDK4 decreased PDH flux and proliferation of attached cells (12). Together with our observations, the effects of PDK4 expression and glucose oxidation differ in attached and suspended cells. Because PDK4 is not expressed in attached mammary cells and is only induced upon cell detachment, it is likely that PDK4 primarily regulates cells in suspension, as it arrests proliferation and, meanwhile, prolongs their viability.

Normal mammary epithelial cells have decreased glucose oxidation in response to detachment in order to survive better in suspension. Because of the Warburg effect, cancer cells constitutively display a low rate of oxidative metabolism of glucose even under attached conditions and therefore are expected to intrinsically possess a survival advantage when detached from matrix. Indeed, cancer cells are resistant to anoikis. Normalization of glucose metabolism in cancer cells by depletion of PDKs or activation of PDH redirects pyruvate toward oxidation in the mitochondria, restores a cancer cell's sensitivity to anoikis, and diminishes the metastatic potential. These findings suggest that the altered glucose metabolism in cancer cells contributes to anoikis resistance and facilitates tumor metastasis. In addition, the results establish PDKs as an important regulator of anchorage-independent cell survival as well as metastatic spread of cancer cells. This may serve as a basis for antimetastasis therapeutic interventions. Reversal of the Warburg effect, in particular inhibition of PDKs to stimulate

glucose oxidation, should render cancer cells susceptible to anoikis and selectively target migrating cancer cells. Such metabolic modulation may impede the detachment of cancer cells from the primary site and eliminate circulating tumor cells as well as disseminated cells at secondary sites before they reestablish conducive cell-matrix interactions.

While normal mammary epithelial cells specifically rely on the ERRγ-PDK4 axis to reprogram metabolism following cell detachment, cancer cells (even under attached conditions) may reduce glucose oxidation through various mechanisms. PDK1 is a direct transcriptional target of hypoxia-inducible factor (HIF) and the oncoprotein Myc, both of which are frequently hyperactivated in cancer (16, 17, 27). Therefore, PDK1 may be broadly upregulated in many cancer cells. PDK2 expression shows a significant correlation with metastasis and is a strong, independent prognostic factor in cervical cancers (24). PDK3 is markedly increased in colon cancer, and its levels are positively associated with the severity of cancer and negatively associated with disease-free survival (23). Microarray studies demonstrated that PDK4 is highly expressed in a subset of cancer cells (30). The genome-wide GISTIC (genomic identification of significant targets in cancer) algorithm (http://www.broadinstitute.org/tumorscape/pages/portalHome.jsf), which recently identified amplification of *PHGDH* in human cancers (22, 29), has also revealed that the *PDK4* locus is significantly focally amplified across the entire data set of over 3,000 human tumors. The significance value for the false discovery rate (FDR) is around $10^{-10}$. The PDK4 amplicon contains about 60 additional genes. It remains to be determined whether amplification of this locus leads to PDK4 overexpression in human cancers and is associated with the metastatic phenotype.

While increased glucose consumption and glycolysis in cancer cells build up glycolytic metabolites to satisfy the anabolic need by cell proliferation (34), it is perplexing why, after glycolysis, the end product pyruvate is predominantly disposed of as secreted lactate rather than converted to acetyl-CoA in the mitochondria under normal oxygen tension. This metabolic shift appears to be an inefficient use of carbon resources, because acetyl-CoA is a major carbon provider and central substrate for fatty acid synthesis. Our study infers that this phenomenon might be attributable to the detrimental consequence of mitochondrial oxidation. Increased glucose consumption through aerobic glycolysis by cancer cells conceivably gives rise to substantially increased pyruvate production. If most pyruvate entered the mitochondrial oxidative pathway as in normal cells, it would generate a huge amount of excess ROS, the by-product of respiratory metabolism. Control of intracellular ROS levels is critical for cancer cell survival. Increased ROS levels may disrupt the cellular redox balance, critically reduce the apoptotic threshold, and jeopardize a cancer cell's capacity to withstand stressful conditions, such as loss of matrix attachment. By diverting pyruvate away from mitochondria, the Warburg effect allows cancer cells to avoid generation of excess ROS and stay in a more reduced state to overcome anoikis. In this regard, increased aerobic glycolysis also shunts more glucose flux into the PPP, which is a principal pathway to generate the reducing equivalent, NADPH (4). NADPH is a major cellular antioxidant that ensures the cell's defenses for detoxification of ROS. By evading overproduction of ROS and elevating the antioxidant program, the Warburg effect maintains redox homeostasis and promotes anoikis resistance and metastasis. Therefore, normalization of glucose metabolism primes cancer cells for anoikis, and antioxidant treatment may enhance metastasis.

It is intriguing that cells activate the ERRγ-PDK4 transcriptional program following matrix detachment. Expression of PDK4 is usually stimulated by starvation, which consequently suppresses PDH and curtails glucose oxidation. This response to fasting conditions conserves glucose reserves and allows the switch from the utilization of glucose to fatty acids as an energy source. On the other hand, ERRs are key regulators of energy metabolism (10). ERRs promote FAO but inhibit glucose oxidation (through upregulation of PDK4) (10). Because FAO and glucose oxidation are mutually inhibitory, which is known as the Randle cycle (15), ERRs may be a key part of mechanisms governing the Randle cycle and fuel selection. It was recently observed that matrix detachment impaired glucose uptake (31). Therefore, cell detachment may mimic glucose starvation and trigger the ERR-PDK4 program and metabolic shift.

This detachment-activated ERR-PDK4 reprogramming axis is reminiscent of the hypoxia-induced HIF-PDK1 pathway (17, 27). Under hypoxia, HIF activates PDK1 to direct glucose metabolites away from the mitochondria, reduce mitochondrial oxygen consumption, and curb toxic ROS generation, thereby helping cells adapt to the hypoxic environment. The HIF-dependent program does not seem to be involved in matrix detachment-induced metabolic reprogramming, as both PDK1 and LDHA, two well-established targets of HIF, did not show changes in expression following cell detachment. Therefore, ERR and HIF share a role in preventing glucose oxidation under different contexts. Indeed, we previously reported that ERR and HIF act collaboratively (1). Because our present study suggests that decreased glucose oxidation dampens anoikis and facilitates tumor cell dissemination, the HIF-PDK1 pathway may not only help cells survive under hypoxia but also contribute to anoikis resistance and metastasis. A hypoxic microenvironment may thus increase the metastatic potential of cancer cells. This is consistent with the notion that intratumoral hypoxia promotes malignant progression (3, 6). Together, these results reinforce that glucose metabolism actively contributes to malignancy.

## ACKNOWLEDGMENTS

We thank Jorg Bungert, Susan Frost, and Mike Kilberg for critically reading the manuscript; Edwards A. Park (University of Tennessee) for kindly providing the PDK4 luciferase reporter construct; and Kevin Brown, Lisa Dyer, and Christiaan Leeuwenburgh for advice and technical assistance.

This work was supported by grants from the National Cancer Institute (R01CA137021) and Florida Bankhead-Coley Cancer Research Program (09BN-12-23092 and 2BT01) to J.L.

We do not have competing financial interests.

## REFERENCES

1. **Ao A, Wang H, Kamarajugadda S, Lu J.** 2008. Involvement of estrogen-related receptors in transcriptional response to hypoxia and growth of solid tumors. Proc. Natl. Acad. Sci. U. S. A. **105**:7821–7826.
2. **Araki M, Motojima K.** 2006. Identification of ERRα as a specific partner of PGC-1α for the activation of PDK4 gene expression in muscle. FEBS J. **273**:1669–1680.
3. **Bertout JA, Patel SA, Simon MC.** 2008. The impact of $O_2$ availability on human cancer. Nat. Rev. Cancer **8**:967–975.
4. **Cairns RA, Harris IS, Mak TW.** 2011. Regulation of cancer cell metabolism. Nat. Rev. Cancer **11**:85–95.
5. **Degenhardt T, et al.** 2007. Three members of the human pyruvate dehydrogenase kinase gene family are direct targets of the peroxisome proliferator-activated receptor beta/delta. J. Mol. Biol. **372**:341–355.

6. **Denko NC.** 2008. Hypoxia, HIF1 and glucose metabolism in the solid tumour. Nat. Rev. Cancer **8**:705–713.
7. **Dufour CR, et al.** 2007. Genome-wide orchestration of cardiac functions by the orphan nuclear receptors ERRα and α. Cell. Metab. **5**:345–356.
8. **Frisch SM, Screaton RA.** 2001. "Anoikis mechanisms." Curr. Opin. Cell Biol. **13**:555–562.
9. **Gatenby RA, Gillies RJ.** 2004. Why do cancers have high aerobic glycolysis? Nat. Rev. Cancer **4**:891–899.
10. **Giguère V.** 2008. Transcriptional control of energy homeostasis by the estrogen-related receptors. Endocr. Rev. **29**:677–696.
11. **Gilmore AP, Owens TW, Foster FM, Lindsay J.** 2009. How adhesion signals reach a mitochondrial conclusion: ECM regulation of apoptosis. Curr. Opin. Cell Biol. **21**:654–661.
12. **Grassian AR, Metallo CM, Coloff JL, Stephanopoulos G, Brugge JS.** 2011. Erk regulation of pyruvate dehydrogenase flux through PDK4 modulates cell proliferation. Genes Dev. **25**:1716–1733.
13. **Hanahan D, Weinberg RA.** 2011. Hallmarks of cancer: the next generation. Cell **144**:646–674.
14. **Hsu PP, Sabatini DM.** 2008. Cancer cell metabolism: Warburg and beyond. Cell **134**:703–707.
15. **Hue L, Taegtmeyer H.** 2009. The Randle cycle revisited: a new head for an old hat. Am. J. Physiol. Endocrinol. Metab. **297**:E578–E591.
16. **Kim JW, Gao P, Liu YC, Semenza GL, Dang CV.** 2007. Hypoxia-inducible factor 1 and dysregulated c-Myc cooperatively induce vascular endothelial growth factor and metabolic switches hexokinase 2 and pyruvate dehydrogenase kinase 1. Mol. Cell. Biol. **27**:7381–7393.
17. **Kim JW, Tchernyshyov I, Semenza GL, Dang CV.** 2006. HIF-1-mediated expression of pyruvate dehydrogenase kinase: a metabolic switch required for cellular adaptation to hypoxia. Cell. Metab. **3**:177–185.
18. **Koppenol WH, Bounds PL, Dang CV.** 2011. Otto Warburg's contributions to current concepts of cancer metabolism. Nat. Rev. Cancer **11**:325–337.
19. **Kroemer G, Pouyssegur J.** 2008. Tumor cell metabolism: cancer's Achilles' heel. Cancer Cell **13**:472–482.
20. **Levine AJ, Puzio-Kuter AM.** 2010. The control of the metabolic switch in cancers by oncogenes and tumor suppressor genes. Science **330**:1340–1344.
21. **Li AE, et al.** 1999. A role for reactive oxygen species in endothelial cell anoikis. Circ. Res. **85**:304–310.
22. **Locasale JW, et al.** 2011. Phosphoglycerate dehydrogenase diverts glycolytic flux and contributes to oncogenesis. Nat. Genet. **43**:869–874.
23. **Lu CW, et al.** 2011. Overexpression of pyruvate dehydrogenase kinase 3 increases drug resistance and early recurrence in colon cancer. Am. J. Pathol. **179**:1405–1414.
24. **Lyng H, et al.** 2006. Gene expressions and copy numbers associated with metastatic phenotypes of uterine cervical cancer. BMC Genomics **7**:268.
25. **Mehlen P, Puisieux A.** 2006. Metastasis: a question of life or death. Nat. Rev. Cancer **6**:449–458.
26. **Orrenius S, Gogvadze V, Zhivotovsky B.** 2007. Mitochondrial oxidative stress: implications for cell death. Annu. Rev. Pharmacol. Toxicol. **47**:143–183.
27. **Papandreou I, Cairns RA, Fontana L, Lim AL, Denko NC.** 2006. HIF-1 mediates adaptation to hypoxia by actively downregulating mitochondrial oxygen consumption. Cell. Metab. **3**:187–197.
28. **Patel MS, Korotchkina LG.** 2006. Regulation of the pyruvate dehydrogenase complex. Biochem. Soc. Trans. **34**:217–222.
29. **Possemato R, et al.** 2011. Functional genomics reveal that the serine synthesis pathway is essential in breast cancer. Nature **476**:346–350.
30. **Ross DT, et al.** 2000. Systematic variation in gene expression patterns in human cancer cell lines. Nat. Genet. **24**:227–235.
31. **Schafer ZT, et al.** 2009. Antioxidant and oncogene rescue of metabolic defects caused by loss of matrix attachment. Nature **461**:109–113.
32. **Semenza GL.** 2011. Hypoxia-inducible factor 1: regulator of mitochondrial metabolism and mediator of ischemic preconditioning. Biochim. Biophys. Acta **1813**:1263–1268.
33. **Tait SW, Green DR.** 2010. Mitochondria and cell death: outer membrane permeabilization and beyond. Nat. Rev. Mol. Cell Biol. **11**:621–632.
34. **Vander Heiden MG, Cantley LC, Thompson CB.** 2009. Understanding the Warburg effect: the metabolic requirements of cell proliferation. Science **324**:1029–1033.
35. **Vaughn AE, Deshmukh M.** 2008. Glucose metabolism inhibits apoptosis in neurons and cancer cells by redox inactivation of cytochrome c. Nat. Cell Biol. **10**:1477–1483.
36. **Wende AR, Huss JM, Schaeffer PJ, Giguère V, Kelly DP.** 2005. PGC-1α coactivates PDK4 gene expression via the orphan nuclear receptor ERRα: a mechanism for transcriptional control of muscle glucose metabolism. Mol. Cell. Biol. **25**:10684–10694.
37. **Zhang Y, et al.** 2006. Estrogen-related receptors stimulate pyruvate dehydrogenase kinase isoform 4 gene expression. J. Biol. Chem. **281**:39897–39906.